



Lawrence Berkeley Laboratory

UNIVERSITY OF CALIFORNIA

Materials & Molecular Research Division

Submitted to Metallurgical Transactions B

WHISKER GROWTH AND SWELLING IN REDUCTION OF OXIDES

Mei Chang and Lutgard C. De Jonghe

January 1983

TWO-WEEK LOAN COPY

*This is a Library Circulating Copy
which may be borrowed for two weeks.
For a personal retention copy, call
Tech. Info. Division, Ext. 6782.*



DISCLAIMER

This document was prepared as an account of work sponsored by the United States Government. While this document is believed to contain correct information, neither the United States Government nor any agency thereof, nor the Regents of the University of California, nor any of their employees, makes any warranty, express or implied, or assumes any legal responsibility for the accuracy, completeness, or usefulness of any information, apparatus, product, or process disclosed, or represents that its use would not infringe privately owned rights. Reference herein to any specific commercial product, process, or service by its trade name, trademark, manufacturer, or otherwise, does not necessarily constitute or imply its endorsement, recommendation, or favoring by the United States Government or any agency thereof, or the Regents of the University of California. The views and opinions of authors expressed herein do not necessarily state or reflect those of the United States Government or any agency thereof or the Regents of the University of California.

WHISKER GROWTH AND SWELLING IN REDUCTION OF OXIDES

Mei Chang* and Lutgard C. De Jonghe*

Lawrence Berkeley Laboratory
University of California
Berkeley, California

This work was supported by the Director, Office of Energy Research,
Office of Basic Energy Sciences, Materials Sciences Division of the
U. S. Department of Energy under Contract No. DE-AC03-76SF00098.

WHISKER GROWTH AND SWELLING IN REDUCTION OF OXIDES

Mei Chang* and Lutgard C. De Jonghe*

Lawrence Berkeley Laboratory
University of California
Berkeley, California

ABSTRACT

Cobalt ferrites were reduced in CO/CO₂ gas mixture at 1173K, at total pressure between 6.6×10^3 Pa and 3.3×10^4 Pa, and at CO/CO₂ ratios between 11.8 and 2.9. Metallic whisker growth was found to be induced by impurities such as CaO and K₂O. The steady state whisker diameter was inversely proportional to the total gas pressure and was relatively insensitive to the CO/CO₂ ratio. A new model is proposed to explain the whisker development. It considers metal-oxide interface diffusion coupled with a metal-oxide-gas triple junction reaction at the whisker base. Whisker formation results for a poorly catalysed triple junction reaction, when metal-oxide interface transport is rapid.

M. Chang is a graduate student, and L. De Jonghe is a Senior Staff Scientist at the Materials and Molecular Research Division, Lawrence Berkeley Laboratory. Dr. L. C. De Jonghe is also Associate Professor-in-Residence at the Department of Materials Science and Mineral Engineering, University of California, Berkeley, CA 94720.

I. INTRODUCTION

The formation of metal alloy whiskers has been known as the cause of extensive swelling of many iron bearing ores during gaseous reduction. The swelling is especially pronounced when CO/CO₂ gas mixtures are used as the reducing agent. An assortment of mechanisms has been invoked to explain this effect. The ore structure and composition,¹⁻⁵ a range of impurities,⁹⁻¹² as well as the reduction conditions^{1,5} all appear to have an effect. It is particularly the impurities that can have a widely varying effect on the reduction product morphology. Some basic oxides including Na₂O, K₂O and CaO enhance the metal nucleation rate and strongly promote iron alloy whisker formation,⁹⁻¹² while MgO, MnO and SiO₂ will not promote whisker growth although they may also enhance the metal nucleation rate. Silica additions are, in fact, used to reduce abnormal swelling during CO/CO₂ reduction of iron ores.¹³ Sulphur also has been found to promote strongly whisker formation, even if H₂/H₂O gas is used as the reducing agent.¹⁴

The reduction reaction mechanisms so far proposed for this type of whisker formation are generally developed along the lines of Wagner's theory on the reduction of non-stoichiometric oxides and sulphides.¹⁵⁻¹⁷ The reducing gas molecule removes oxygen from the exposed oxide surface, and the excess cations that are produced there combine with cation vacancies or fill interstitial sites. If Fe³⁺ is present it will be reduced to Fe²⁺. The excess cations are then transported to a nearby sink - a metal/oxide interface - and converted to metal. Metal alloy nucleation considerations are then coupled with the Wagner mechanism. Impurity build-up at the whisker/oxide/gas triple junction are often

involved to explain the arrest of the whisker diameter growth. These theories can, however, not readily account for two significant features of whisker formation: one is that whisker formation depends on the chemical composition of the gas and not just on the equivalent oxygen partial pressure; a second one is that a quasi-steady whisker diameter develops that - as will be shown in this report - can increase or decrease depending on the reduction conditions. We will argue that an essential aspect of the reduction reactions is the removal of oxygen from the metal/oxide interface under the whisker, and that it in this mechanism, together with catalytic processes at the gas/metal/oxide junction at the whisker base, that controls the morphology of the metallic alloy reduction product.

II. EXPERIMENTAL PROCEDURE

The alloy oxide 99% dense, polycrystalline cobalt ferrites were prepared by Countis Industries.* This material contains about 0.06 wt% NiO, as well as impurities below the 100 ppm level. Specimens were cut from the oxide, with dimensions of 10mmx10mmx1mm. One side of the specimens was ground and polished with 0.03 μ m diamond paste. For some specimens surface damage induced by the polishing was removed by argon ion sputtering at 7 kV, for about 30 min.

*P.O. Box 1444, San Luis Obispo, California

Some specimen surfaces were intentionally contaminated with calcium or potassium prior to reduction. These specimens were dipped in a saturated Ca(OH)_2 or in a $2.5 \times 10^{-2} \text{M}$ KOH solution and dried. These specimens were termed "heavily contaminated". For other specimens the solution was removed from the surface by an air jet before drying; this left much less Ca or K iron on the surface. These specimens were termed "lightly contaminated". Comparison of the reduction product morphologies of these specimens with those that were not intentionally contaminated would permit a qualitative assessment of the role of the Ca^{++} and K^+ impurities.

The specimens were suspended in a quartz tube for the reduction experiment. They were heated up in air at about 13 Pa, to the desired temperature, and then the reducing gas was introduced rapidly at a controlled pressure. The reducing conditions established in about 30 sec. The gas flow rate was sufficiently high to avoid any gas starvation effects. For some experiments the gas pressure was rapidly changed to a new level during reduction. This permitted the observation of the morphological changes resulting from such treatments, on the same whiskers. After reduction the specimens were quenched by causing them to drop on a copper cooling block. The quenching treatment was necessary to preserve the metal alloy whiskers without reoxidation.

The product morphology was studied with a scanning electron microscope (SEM) and stereo pair micrographs were taken. The morphology of the metal/oxide interface was also examined by SEM, after the whiskers were removed by etching partly reduced samples with a 10% Br_2 solution in methanol, for 1 minute.

III. RESULTS

The general appearance of a specimen briefly reduced at 1173K in $\text{CO}/\text{CO}_2 = 10$ is shown in Fig. 1. The growing metal whiskers have lifted not yet completely reduced grains of oxide, and have tangled where the whisker density is high. The separation between the different grains in the substrate is in good agreement with what is expected from the spinel \rightarrow wustite transformation and from continued reduction. The separation increases with reduction time and can thus yield the approximate rate at which gas/oxide interface recedes. The average gas/solid interface velocity at times less than 10 min was found to be about 5×10^{-9} m/sec, corresponding to an oxygen flux of about 5×10^{-4} g atom $\text{O}/\text{m}^2\text{sec}$. The oxide surface becomes pitted and faceted during the reduction, as is shown in Fig. 2. The faces of the pits appear to be $\{111\}$ planes, corresponding to the densest oxygen planar packing in these cubic oxides. Figure 2 shows that the whiskers also tends to facet. The metal/oxide interface under the whisker is revealed in Fig. 3. Here, the same whiskers bases were located after the metal had been removed with the bromine solution. The stereo pair micrograph, Fig. 3c and 3d, shows that the metal/oxide interface is again faceted and that it is quite close to the surrounding surface. The tendency for faceting strongly suggests that selected orientation relationships occur between the metal whisker and the matrix. Such orientation relationships were studied earlier for reduction of cobalt ferrite by De Jonghe and Thomas.¹⁸

For polished and ion sputtered surfaces, metal is nucleated preferentially near the grain boundaries or near pores within a grain,

as shown in Fig. 4. Examination of intergranular fracture surfaces with the scanning Auger microscope shows that the grain boundaries and pore surfaces are enriched in impurities much as Ca and Na as shown in Fig. 5. Auger microscopy also showed some S on pore surfaces. The preferred formation of metal at grain boundaries and pores of sputter-cleaned specimens thus indicated that impurities such as Ca, Na, and S stimulate metal nucleation. Whisker growth in lightly contaminated specimen surfaces are shown for Ca ion, Fig. 6a, and K ion, Fig. 6c, surface contamination. Whisker formation is now more uniform over the surface. For heavily Ca or K ion contaminated surfaces the whisker density increases dramatically, as shown in Figs. 6b and 6d. The impurities also appear to lead to thinner whiskers.

Variations in whisker diameter were observed for a given specimen, and were probably due to variations in local impurity concentrations and in metal/oxide interfacial structure. The experiments in which the total pressures were changed during the course of reduction permitted the evaluation of the change in whisker diameter on the same whisker. Figure 8 shows the whisker diameter change for a specimen reduced at 1173K for 180 sec at 1.3×10^4 Pa, followed by a 240 sec reduction at 0.66×10^4 Pa, at a constant $\text{CO}/\text{CO}_2 = 11.8$. The whisker diameter increases significantly when the total pressure is reduced at constant CO/CO_2 . The opposite is the case for reduction in which the pressure is stopped up, with a constant $\text{CO}/\text{CO}_2 = 11.8$, during reduction. Figure 9 shows the change in whisker diameter for a specimen reduced at 1173K, for 360 sec at 0.66×10^4 Pa, followed by reduction for 30 sec at 2.6×10^4 Pa. In this experiment the whiskers tended to cluster, but

the decrease in whisker diameter with increasing total gas pressure is quite evident. The whisker diameter ratios after total gas pressure changes are shown in Fig. 9. These results indicate that the whisker diameter is proportional to the inverse of the total gas pressure.

At constant total pressure the whisker diameter was relatively insensitive to R_g within the range tested. If R_g was changed from 12 to about 3, less than 20% change in whisker diameter was observed. Even smaller changes were observed in whisker diameter when R_y was changed at constant CO pressure.

IV. DISCUSSION

When oxide is reduced to metal, the metal/oxide interface must advance. In Fig. 3 it was shown that this metal/oxide interface under the whisker remains close to the oxide/gas interface. Thus, oxygen must be removed from the whisker/oxide interface at a rate that is compatible with the rate with which the surrounding oxide/gas interface recedes. This rate was about 5×10^{-4} g atom O/m²sec.

The axial growth of the whisker is determined by the oxide/gas interface velocity, the whisker diameter, and the average whisker spacing. The diameter of the whisker is determined by a balance between reactions and transport processes at the whisker base, as discussed now.

Oxygen from the advancing metal whisker/matrix oxide interface can be removed by three mechanism: oxygen diffusion through the metal whisker, through the oxide bulk, or along the metal/oxide interface. The maximum expected oxygen flux, J_{\max} , can be estimated to within one or two orders of magnitude from $J_{\max} = -C \cdot \beta \cdot D \Delta \mu_{\max} / kT\lambda$, where C

is the oxygen concentration, D is the oxygen diffusion coefficient, β is a geometrical parameter equal to the thickness of the equivalent circular slab through which oxygen transport near the whisker base occurs, $\Delta\mu_{\max}$ is the maximum oxygen chemical potential difference between the oxygen source and sink, and λ is a distance on the oxide of the whisker radius R . For volume diffusion processes one could also estimate β to be on the order of the whisker radius; for interface diffusion β would become equal to the interface "thickness" and would be on the order of a few lattice parameters. In a cylindrical geometry, one should have, in the steady state, that $J_{\max} = C_0 v R / 2$, since $\pi R^2 C_0 v = 2\pi R J_{\max}$, where C_0 is the oxygen concentration in the oxide. Since v was measured to be about $5 \times 10^{-9} \text{ m/sec}$, J_{\max} should be about $5 \times 10^{-4} \text{ g atom O/m}^2 \text{ sec}$. Then, putting $\Delta\mu_{\max} = kT \cdot \ln(p_{\text{O}_2}^e / p_{\text{O}_2}^g)^{1/2}$, where experimentally $p_{\text{O}_2}^e / p_{\text{O}_2}^g = 100$, and $\beta \approx \lambda \approx 10^{-6} \text{ m}$, then require $C D > 2.5 \times 10^{-11} \text{ C} \cdot D > 2.5 \times 10^{-11} \text{ g atom O/m sec}$.

Oxygen diffusion through the oxide is expected to be very slow; if it is estimated that the O^{2-} diffusion coefficient in the wustite is comparable to that in CoO , measured by Chen and Jackson,¹⁹ then $D \approx 10^{-20} \text{ m}^2/\text{sec}$ around 1173K, which $C \approx 1 \times 10^5 \text{ g atom O/m}^3$. Clearly, oxygen diffusion through the oxide phase is not a likely mechanism. Oxygen transport data for the FCC Fe-Co alloys that constitute the whiskers are not available. For FCC iron, at 900°C , the solubility limit is around 2 ppm,²⁰ so that is now about $6 \times 10^{-1} \text{ g atom O/m}^3$, with $D \approx 3 \times 10^{-11} \text{ m}^2/\text{sec}$.²⁰ This gives $C \cdot D \approx 2 \times 10^{-11} \text{ g atom O/m sec}$. For FCC cobalt at 800°C , D might be extrapolated from diffusion data obtained by Grundy and Nolan²¹ giving $D \approx 3 \times 10^{-13} \text{ m}^2/\text{sec}$. C for cobalt was deter-

mined by Seybolt et al.²² and is about 6×10^{-1} g atom O/m³ at the solubility limit, around 1173K. This gives again $C \cdot D \approx 2 \times 10^{-11}$ g atom O/cm sec. Since there are significant uncertainties in the estimates of the parameters, the correspondence of these values to the experimental value of $C \cdot D$ is fortuitous. Oxygen transport from the metal/oxide interface through the whisker bulk metal might thus be possible. No data are available for oxygen transport along the metal/oxide interface at the whisker base, but results on hydrogen reduction of cobalt ferrites, reported by Porter and De Jonghe,²³ suggest that it can be very fast. Interface oxygen transport is thus also a possible mechanism. Which of the two mechanisms is dominant may be decided on the basis of the morphology of the dense metal reduction product that forms on pure wüstite reduced with CO/CO₂, at 1173K, for 180 sec, Fig. 10. The very flat geometry of the formed metal cannot be obtained when oxygen diffusion through the metal is dominant. Indeed, a lenticular shaped product should develop, as shown qualitatively in Fig. 11. The rate of radial growth of the metal layer the surface, L , is controlled by a chemical reaction, since diffusional processes very near the junction metal edge can no longer be rate controlling. L should then be approximately constant. This would lead to a metal product phase profile, assuming parabolic layer thickness growth kinetics, described approximately by $y = D[t - (r/L)]^{1/2}$. This is not observed. When metal/oxide interface transport is dominant, a flat product phase morphology should be expected. A detailed analysis of this transformation morphology development permits evaluation of the oxygen interface transport rate, and will be reported later. It is therefore concluded that oxygen trans-

port along the metal/oxide interface is, in fact, the dominant mechanism during reduction of the oxides under consideration here.

During the whisker growth formation a quasi-steady state prevails, and the metal/oxide interface advances with a rate, v , determined by the overall reaction rate at the gas/oxide interface. The rate of oxygen removal from under the whisker must then equal the rate of the gas/solid reaction at the metal/oxide/gas triple junction, J_R . Referring to Fig. 12, one has in cylindrical coordinates:

$$J_{B\delta} = -D_{B\delta} C_O \nabla_r \mu / kT \quad (1)$$

Since a quasi steady state is assumed, one also has

$$\nabla_r \cdot (J_{B\delta}) = C_O v \quad (2)$$

or

$$\nabla_r^2 \mu_O = -kTv/D_{B\delta} \quad (3)$$

with

$\nabla_r \mu_O = 0$ at $r = 0$, $\mu_O = \mu_T$ at $r = R$, and $\mu_O = \mu_e$ at $r = 0$, this yields

$$\mu_O = \mu_T + \frac{kT}{4D_{B\delta}} v (R^2 - r^2) \quad (4)$$

Equation (4) with $\mu_O = \mu_e$ at $r = 0$ gives

$$R^2 = 4D_{B\delta} (\mu_e - \mu_T) / kTv \quad (5)$$

The radius of the whisker will depend on the oxygen chemical potential established at the triple junction, μ_T , on the oxygen solid state transport rate, and on the reduction rate, v . μ_T is between μ_g and μ_e , and depends on the gas/solid reaction rate and mechanism at the whisker base. This will, in turn, depend on the local catalysis process, which can be strongly affected by the gas composition and by the surface impurities. For a well catalyzed, rapid reaction $\mu_T \approx \mu_g$,

and the whisker diameter is oxygen interface diffusion controlled. This would give the maximum whisker diameter with $R \propto v^{1/2}$. At the gas pressures used in the present experiments, v is proportional to P ,²³ so that $R \propto P^{1/2}$ would be expected. For a poorly catalyzed reaction, the triple junction reaction becomes rate controlling, and μ_T approaches μ_e , giving small diameter whiskers. One may also write for the quasi-steady state:

$$2\pi R J_R = \pi C_O R^2 v \quad (6)$$

where J_R is the gas/solid reaction rate at the triple junction, so that with Eq. (5)

$$(\mu_e - \mu_T) = kT J_R^2 / D_B \delta v C_O^2. \quad (7)$$

For gas/solid reactions J_R will probably follow Langmuir-Hinshelwood kinetics, ranging between linear and constant as a function of gas pressure. Thus $(\mu_e - \mu_T)$ would be proportional to v for $J_R \propto v$, and proportional to $1/v$ for $J_R = \text{constant}$, since v is proportional to P . In these two limiting cases, Eq. 5 predicts that one would observe $R = \text{constant}$ or $R \propto 1/P$. Figure 9 shows that the average whisker diameter as a function of total gas pressure at $R_g = \text{constant}$ was inversely proportional to P , supporting a reaction mechanism with J_R constant. Impurities such as S strongly promote whisker formation,¹⁴ and S is known to be strongly absorbed on metal but not on oxide, so it is reasonable to assume that the relevant catalytic processes occur on the metal rather than on the oxide surface. These possible species can then be considered for removing oxygen from the triple junction:

- 1) gaseous CO: CO(g) ; 2) molecularly adsorbed CO: CO(ma) ; and 3) dissociatively adsorbed CO, i.e. carbon: CO(da) . If CO(g) were controll-

ing the reaction, then J_R would have to depend on P . Since this was not observed, direct oxygen removal by CO(g) is not expected. Oxygen removal by CO(ma) at incomplete surface coverage would give the same result and can also be eliminated. Thus, either CO(ma) or CO(da) , at near complete coverage, would seem to be the species involved in the rate controlling reaction. At the temperatures and gas pressures used here only strongly adsorbed species can give a significant degree of surface coverage. From the work of Benzinger and Madix,²⁵ it is clear that CO(ma) coverage in iron, and thus likely also on Fe-Co alloys, can only be expected to be small above 400K, thus leaving the more strongly bound CO(da) as the next likely species involved in the rate controlling triple junction reaction. Since this reaction appeared to be nearly independent of the gas pressure, it would have to be assumed that the CO(da) is in near saturation. This corresponds effectively to the pressure of a surface carbide. Such a surface carbide would not be unreasonable in view of the strong CO(da) adsorption.²⁵ CO_2 adsorption is unlikely to be involved in the rate controlling triple junction reaction, since it is known to be a weakly adsorbed species on metals.²⁶

In a first approximation, one could express the reaction velocity, v , as a first order reaction:

$$v = B' [\text{CO(g)}], e' [\text{CO}_2(\text{g})]. \quad (8)$$

Thus, since $P = [\text{CO(g)}] + [\text{CO}_2(\text{g})]$ and with $[\text{CO(g)}]/[\text{CO}_2(\text{g})] = R_g$, one has that

$$v \propto \left(1 - \frac{R_g^*}{R_g}\right) P / \left(1 + \frac{1}{R_g}\right) \quad (9)$$

where R_g° is the metal-oxide equilibrium value of R_g . Combination of Eqn. (9) and Eqn. (6), with J_R constant, thus would predict that R would be relative insensitive to the range of R_g values and hence, at constant P , since R_g was several times larger than R_g° . The experimental observation of the relative insensitivity of the whisker radius to changes in R_y at constant P are in agreement with this prediction.

One last point that merits discussion is the atomic mechanism by which the whiskers changes diameter when the gas pressure is changed. Clearly, the changes in whisker diameter cannot be explained on the basis of arrested growth after nucleation. The changes in whisker diameter can, however, be understood if we consider their increasing or decreasing diameter together with the interface oxygen removal. A schematic series of drawings, Fig. 13, illustrates how the diameter changes may be accomplished simply when the quasi-steady state has not yet been reached. The shaded area in this figure indicates where oxygen has been removed. This model implies that the radial growth of the whisker also involves a reduction reaction.

V. CONCLUSIONS

Whisker growth during CO/CO_2 reduction of cobalt ferrites, and likely other iron bearing oxides, is due to oxygen transport limitation from under the advancing metal/oxide interface. The transport limitation is caused by ineffective catalytic processes at the metal/oxide/gas junction in CO/CO_2 reduction.

VI. ACKNOWLEDGEMENTS

This work was supported by the Division of Materials Sciences, Office of Basic Energy Sciences of the U. S. Department of Energy under Contract No. DE-AC03-76SF00098.

References

1. T. Fuwa and S. Ban-Ya: Trans. ISIJ, 1969, Vol. 9, 137-47.
2. E. Mazanek, S. Jasienska, and C. Bryk: Arch. Eisenhuttenwes., 1979, Vol. 50, 57-62.
3. A. Ischimitsu: Tetsu-To-Hagane, Overseas, 1965, Vol. 5, 214-16.
4. N. Ponghis, R. Vidal, A. Bargard, and A. Poos: Iron making Proc., Met. Soc. AIME, 1967, Vol. 26, 146-56.
5. M. C. Chang, J. Vlnaty and D. Kestner: ibid., 140-45.
6. W.-K., Lu, Scan. J. Metallurgy: 1973, Vol. 2, 273-76.
7. W.-K., Lu: ibid, 169-72.
8. W. Wenzel, and H. W. Gudenau: Stahl u. Eisen, 1970, Vol. 13, 689-97.
9. Tel. L. Kasabgy, and W.-K. Lu: Met. Trans., 1980, Vol. 11B, 409-14.
10. A. Schneider, and K. Koch: Arch. Eisenhuttenwes., 1979, Vol. 50, 281-88.
11. R. L. Bleifuss: Trans. SME/AIME, 1970, Vol. 247, 225-31.
12. J. F. Grandsen, and J. S. Sheasby: Can. Metall. Quart., 1974, Vol. 13, 479-84.
13. W.-K. Lu: Scan. J. Metallurgy., 1974, Vol. 3, 49-55.
14. H. de Haas, K. Grebe, and F. Oeters: Arch. Eisenhuttenwes., 1980, Vol. 51, 167-72.
15. R. Nicholle, and A. Rist: Met. Trans., 1970, Vol. 10B, 429-38.
16. C. Wagner: J. Metals, 1952, Vol. 4, 214-16.
17. C. Wagner: Steelmaking: The Chipman Conference, 1969, 19-26.
18. L. C. De Jonghe and G. Thomas: Mater. Sci. Eng. 1971, Vol. 8, 259-74.

19. W. K. Chen, and R. A. Jackson: J. Phys. Chem. Solids, 1969, Vol. 30, 1309-14.
20. J. H. Swisher, and E. T. Turkdogan: Trans. Met. Soc. AIME, 1967, Vol. 239, 426-31.
21. P. J. Grundy, and P. J. Nolan: J. Mat. Sci., 1972, Vol. 7, 1086-87.
22. A. U. Seybolt, and C. H. Mathewson: Trans. AIME, 1935, Vol. 117, 156-72.
23. J. R. Porter, and L. C. De Jonghe: Met. Trans., 1981, Vol. 11B, 299-309.
24. K. H. Ulrich, K. Bohnenkamp, and H. J. Engell: Arch. Eisenhuttenwes., 1965, Vol. 9, 611-18.
25. J. Benzinger, and R. J. Madix: Surface Sci., 1980, Vol. 94, 119-53.
26. G. C. Bond, "Heterogeneous Catalysis: Principles and Applications", Clarendon Press, Oxford, 1974, pp. 21-23.

Figure Captions

Fig. 1. Stereo micrograph of cobalt ferrite reduced in $\text{CO}/\text{CO}_2 = 10$.

Some partly reduced grains have been lifted off the surface. Metal whiskers tangle where their density is high. The separation between the grains in the substrate is due to the spinel \rightarrow wüstite transformation as well as to further wüstite reduction.

Fig. 2. Metal whisker and pitting of the oxide surface. The pit facets are $\{111\}$ planes. The metal whisker also tends to facet.

Fig. 3. The whiskers (1173K, $\text{CO}/\text{CO}_2 = 11.8$, $0.66 \times 10^4 \text{ Pa}$, 300 sec) in figure a, have been removed by etching with 10% Br_2 -methanol for 1 min in figure b. The area boxed in figure b is shown enlarged in the stereo pair figures c and d. The metal/oxide interface under the whiskers, shown in figures c and d, is slightly below the neighboring surface, and also tends to facet.

Fig. 4. For polished and ion sputtered surfaces, whisker nucleation is confined to the grain boundary areas.

Fig. 5. Intergranular fracture surfaces of the cobalt ferrites.

Figure a is an SEM image of the same area shown by Ca mapping in figure b and by Na mapping in figure c with the scanning Auger microscope.

Fig. 6. a) Whisker formation on "lightly" Ca contaminated surface.

b) Whisker formation on "heavily" Ca contaminated surface.

c) Whisker formation on "lightly" K contaminated surface.

d) Whisker formation on "heavily" K contaminated surface.

All specimens were deduced at 1173K with $\text{CO}/\text{CO}_2 = 11.8$, at a total gas pressure of $1.3 \times 10^4 \text{ Pa}$.

Fig. 7. Stereo pair of whisker diameter change for a specimen reduced at 1173K for 180 sec at 1.3×10^4 Pa followed by a 240 sec reduction at 0.66×10^4 Pa, at $\text{CO}/\text{CO}_2 = 11.8$. The whisker diameter changes by about a factor of 2.

Fig. 8. Stereo pair of whisker diameter change for a specimen reduced at 1173K, for 360 sec at 0.66×10^4 Pa, followed by a reduction for 30 sec at 2.6×10^4 Pa. The whisker splits up into several smaller diameter whiskers.

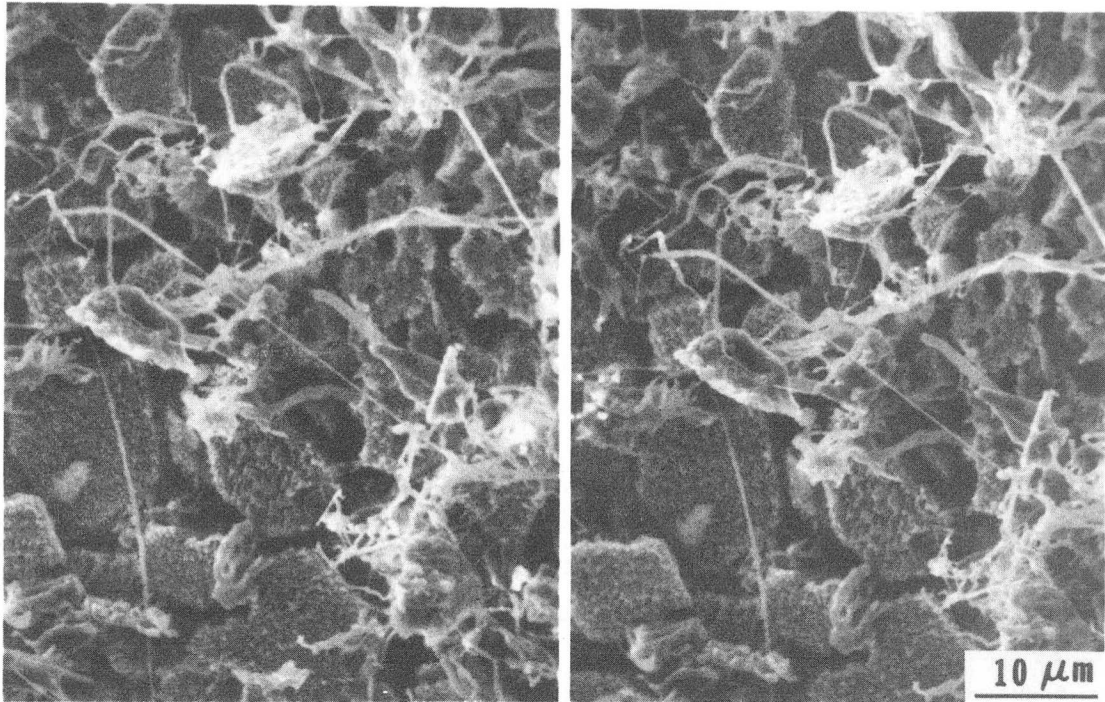
Fig. 9. Whisker diameter ratio as a function of total gas pressure ratio for experiment of the type shown in Figs. 7 and 8.

Fig. 10. Morphology of dense iron formed on dense FeO after reduction at 1173K, for 180 sec, with $\text{CO}/\text{CO}_2 = 11.8$. The iron forms as a thin layer that spreads radially over the surface of the oxides.

Fig. 11. Geometry of dense Fe on FeO expected when oxygen diffusion through the dense Fe product would be rate controlling. L is the radial growth rate of the Fe.

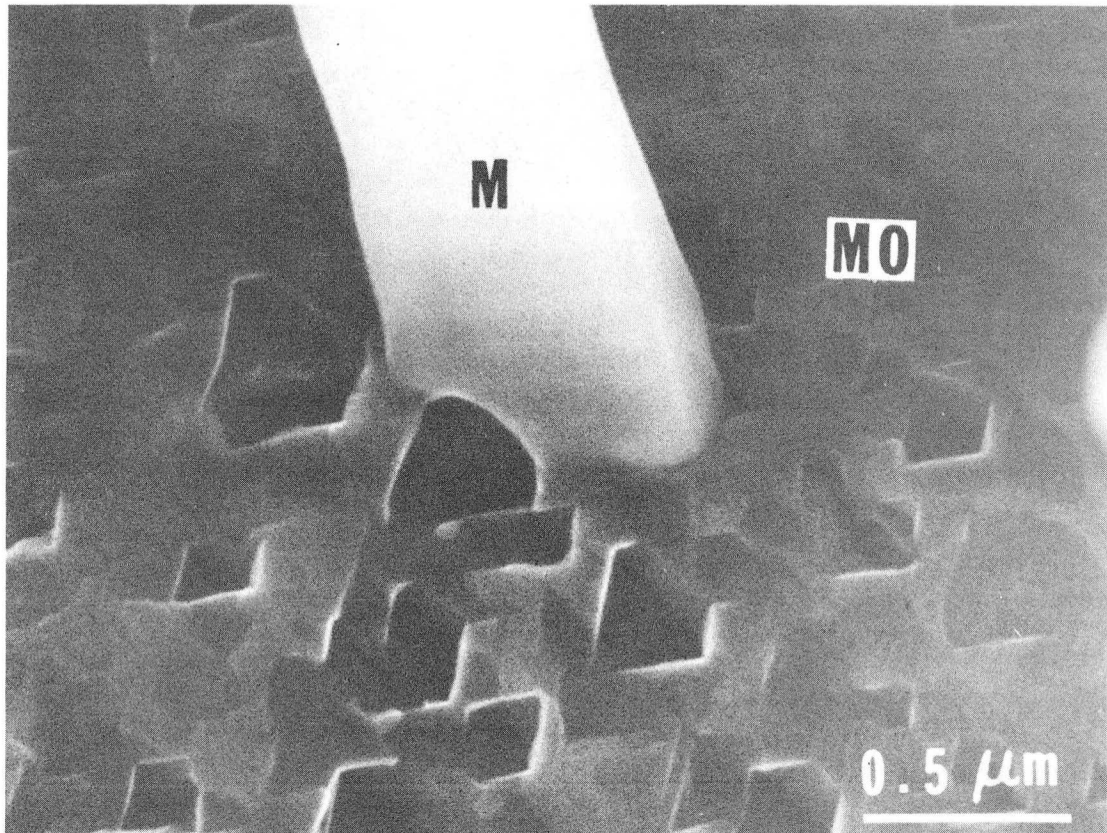
Fig. 12. Whisker geometry. The oxide/gas interface is advancing with a velocity v .

Fig. 13. Schematic illustration of the mechanism by which the changes in whisker diameter can occur. The shaded area is the new metal formed. The axial growth at rate, \dot{a} , is accomplished by supply of metal ions from the neighboring metal/oxide interface.



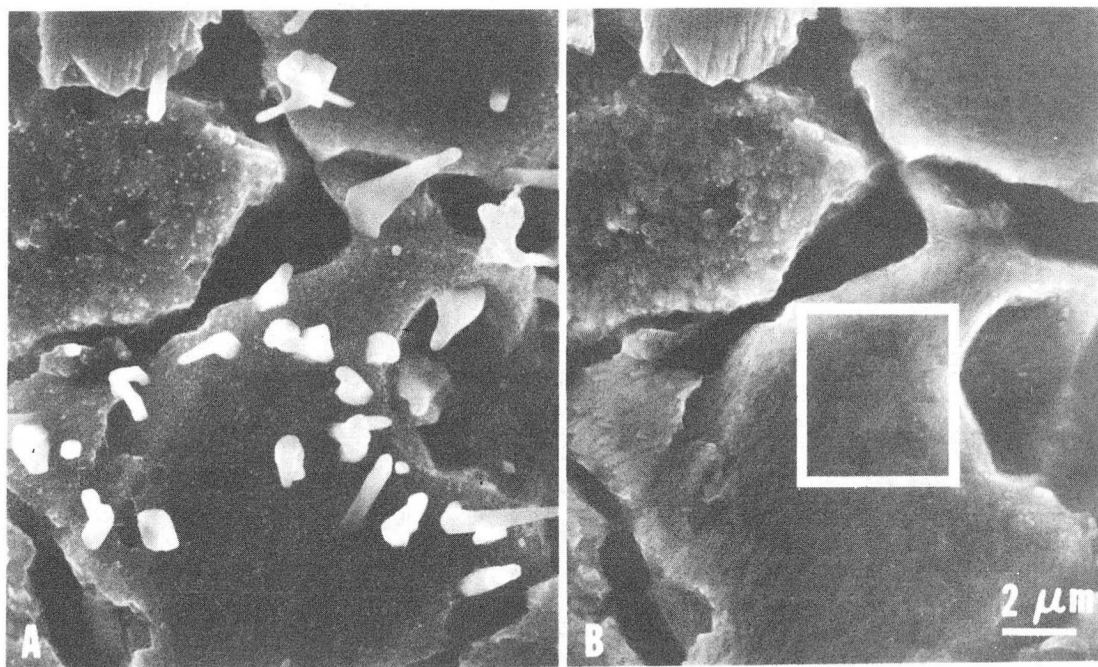
XBB 832-1118

Fig. 1



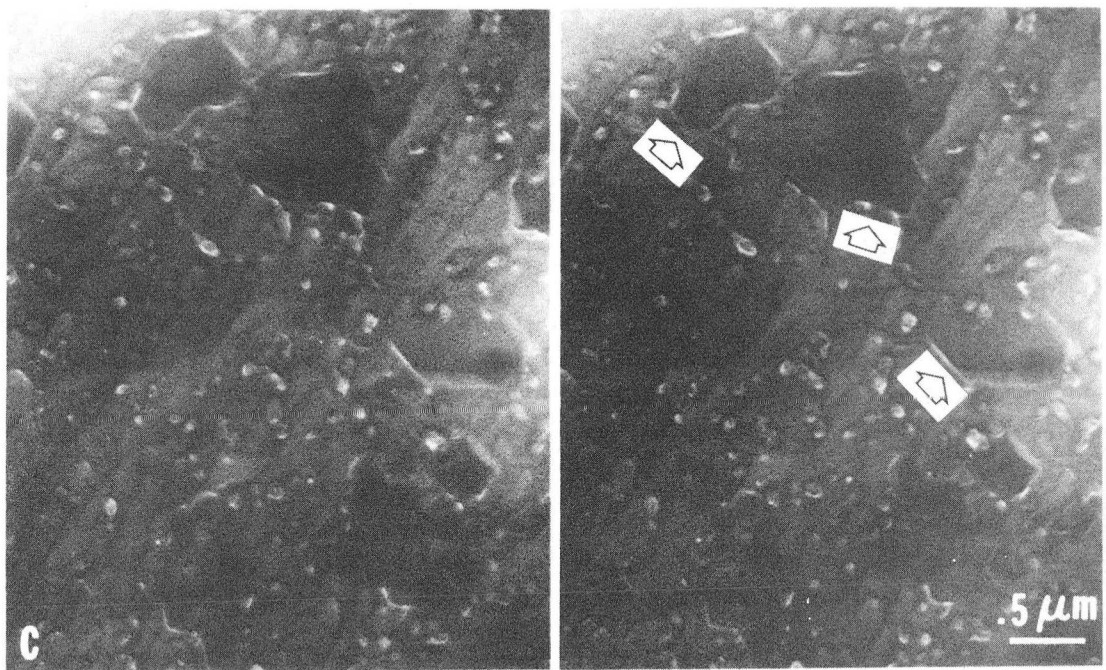
XBB 819-8722A

Fig. 2



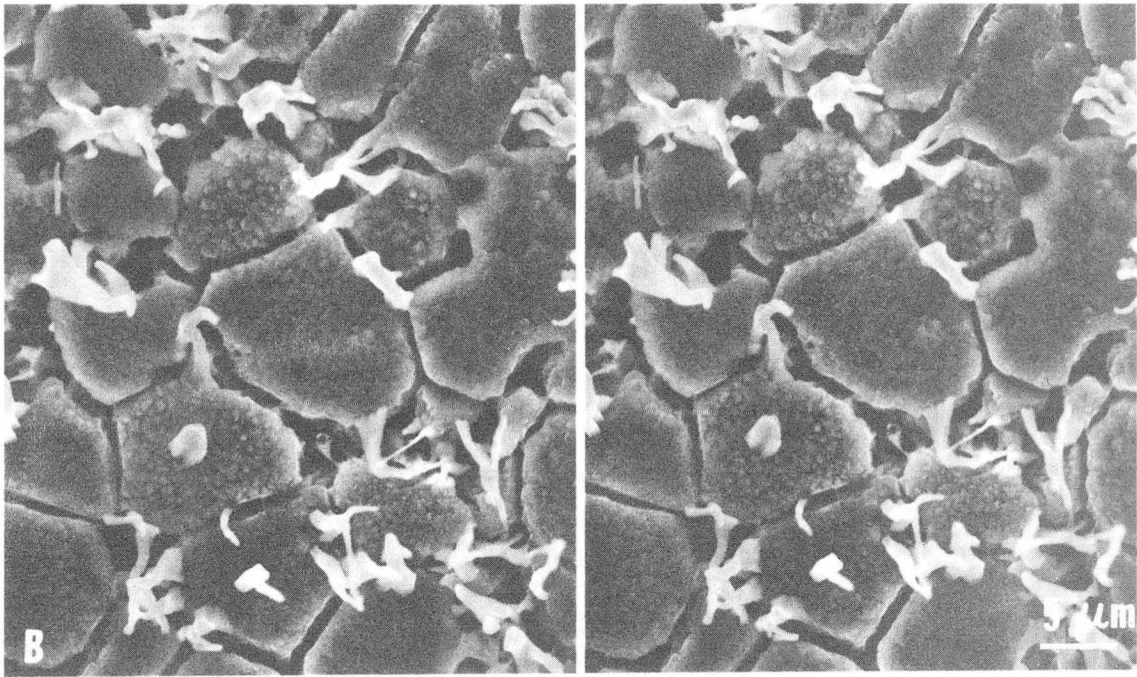
XBB 832-1113

Figs. 3 A,B



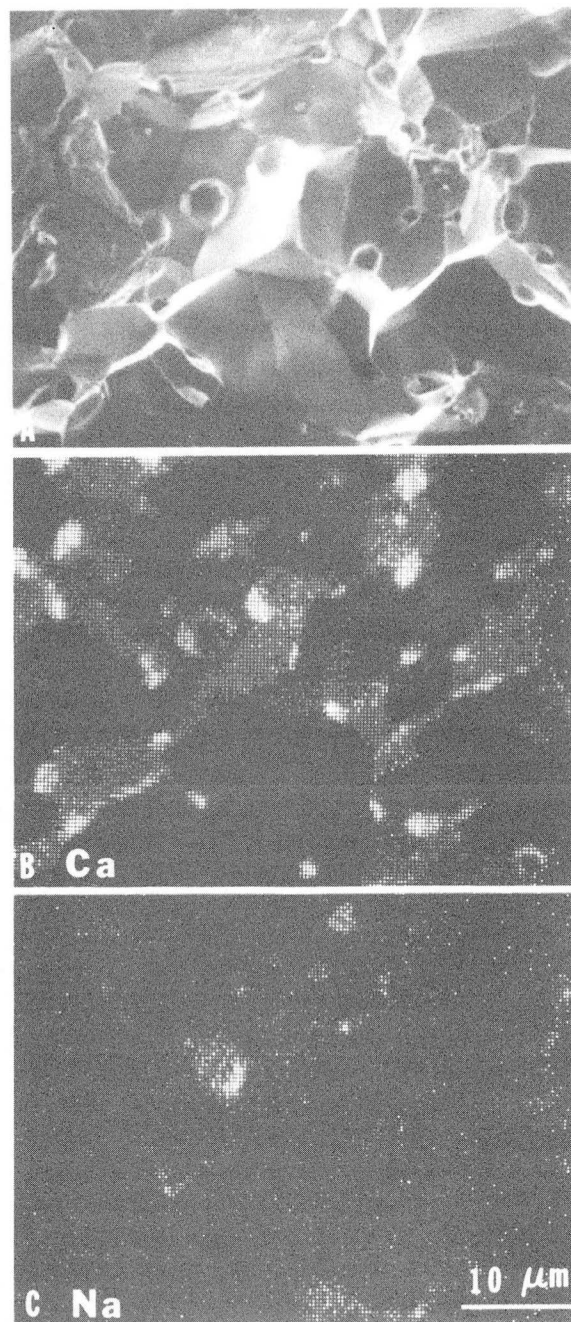
XBB 832-1114

Fig. 3C



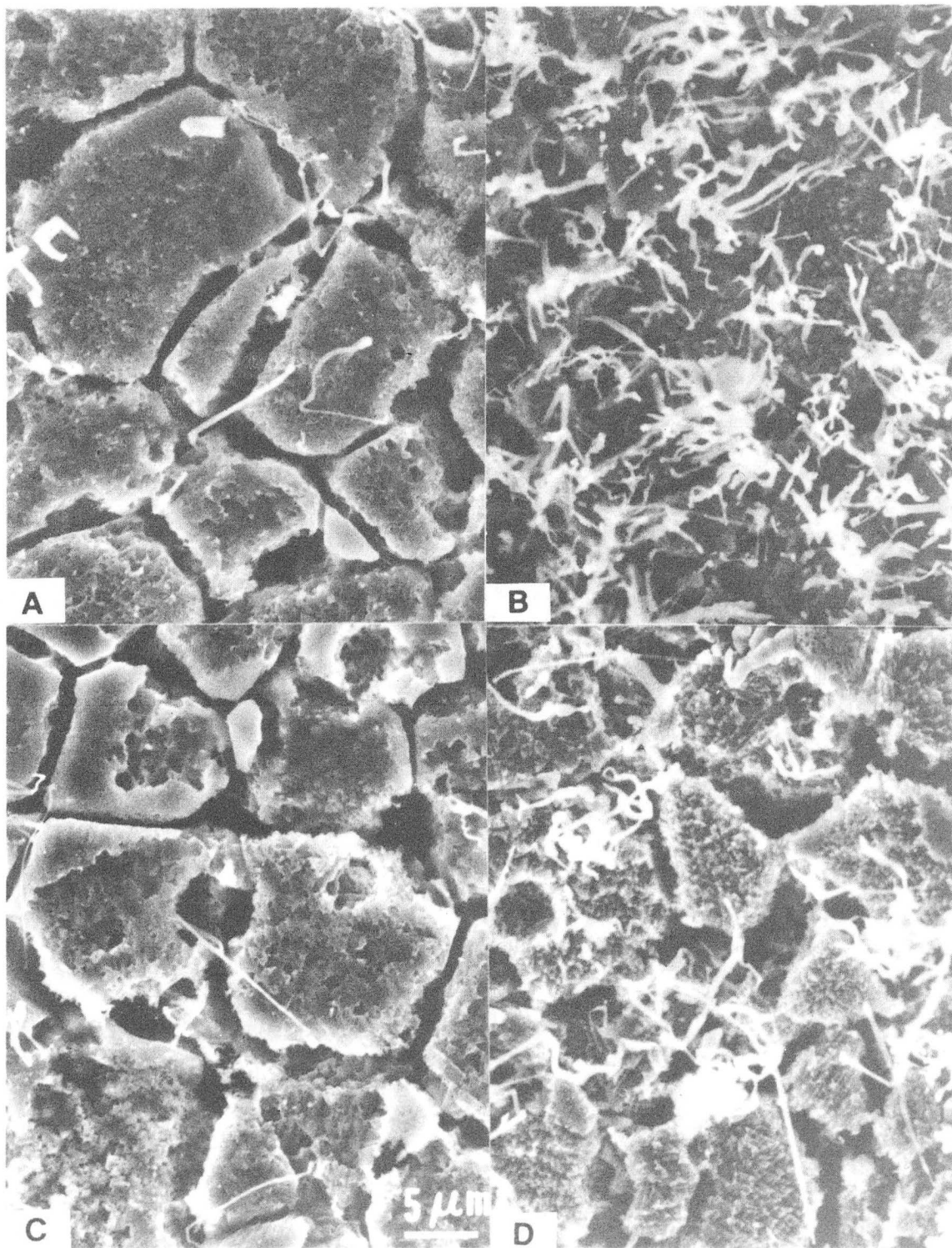
XBB 832-1106

Fig. 4



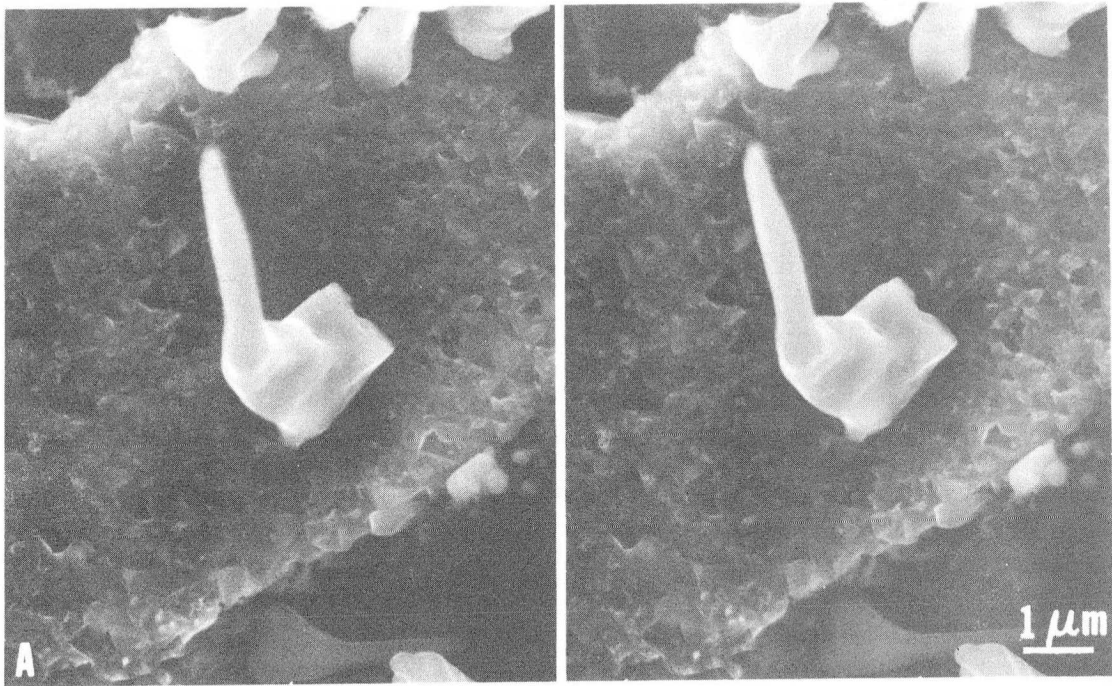
XBB 832-1117

Fig. 5



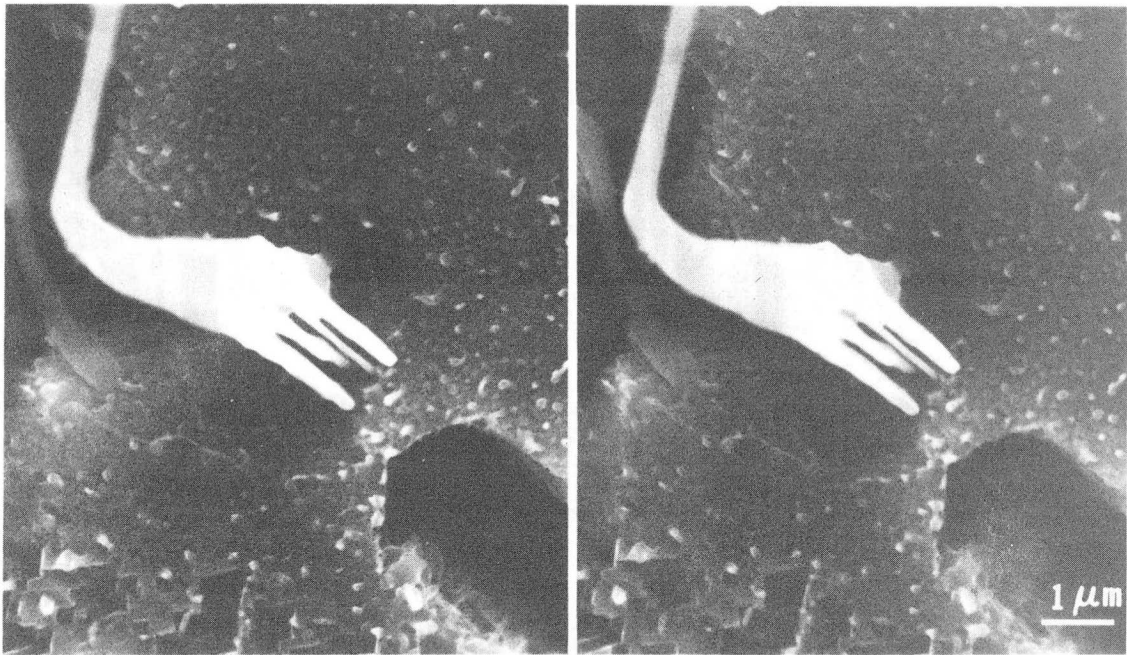
XBB 834-3276

Figs. 6 A,B,C,D



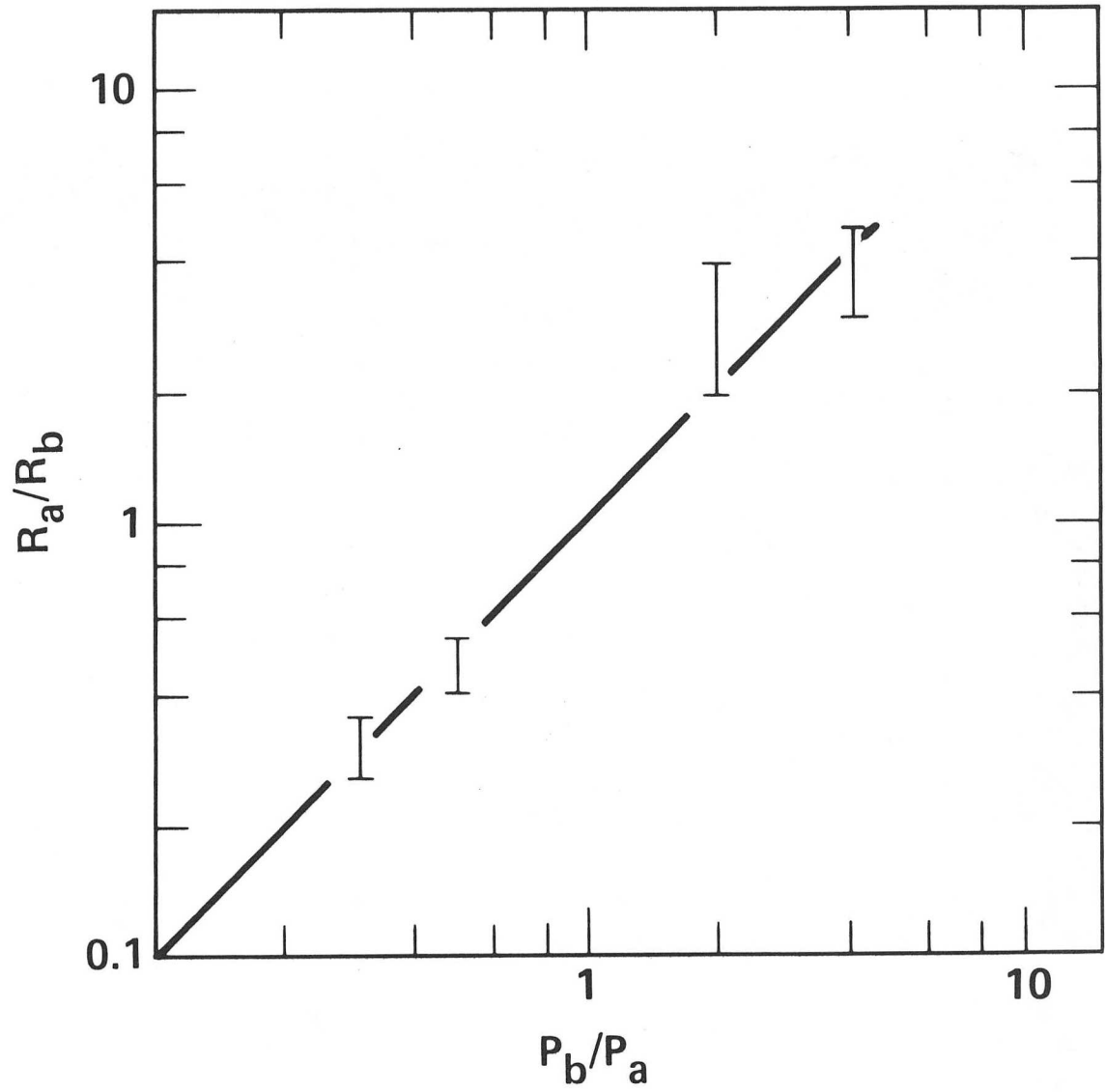
XBB 832-1107

Fig. 7



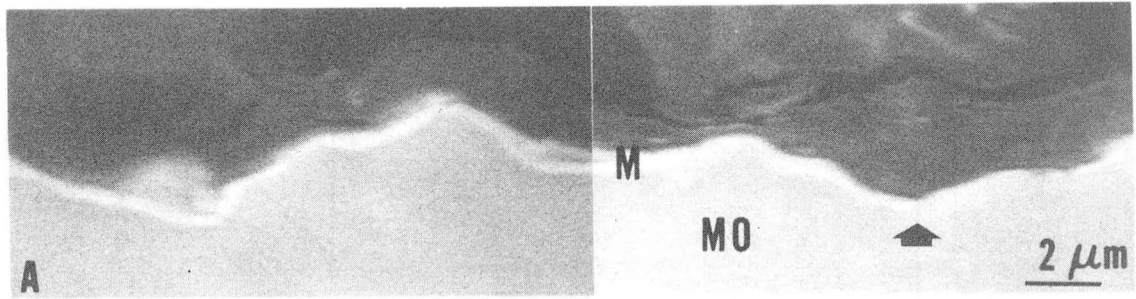
XBB 832-1115

Fig. 8



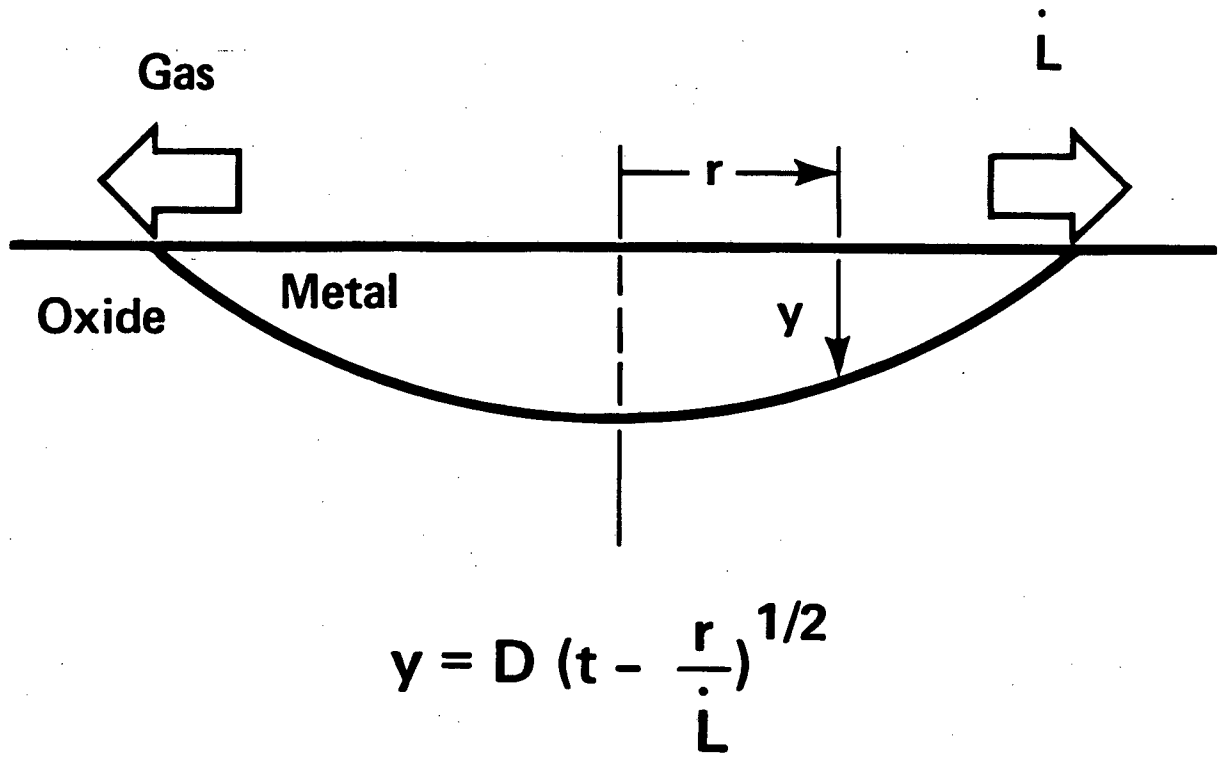
XBL 831-1143

Fig. 9



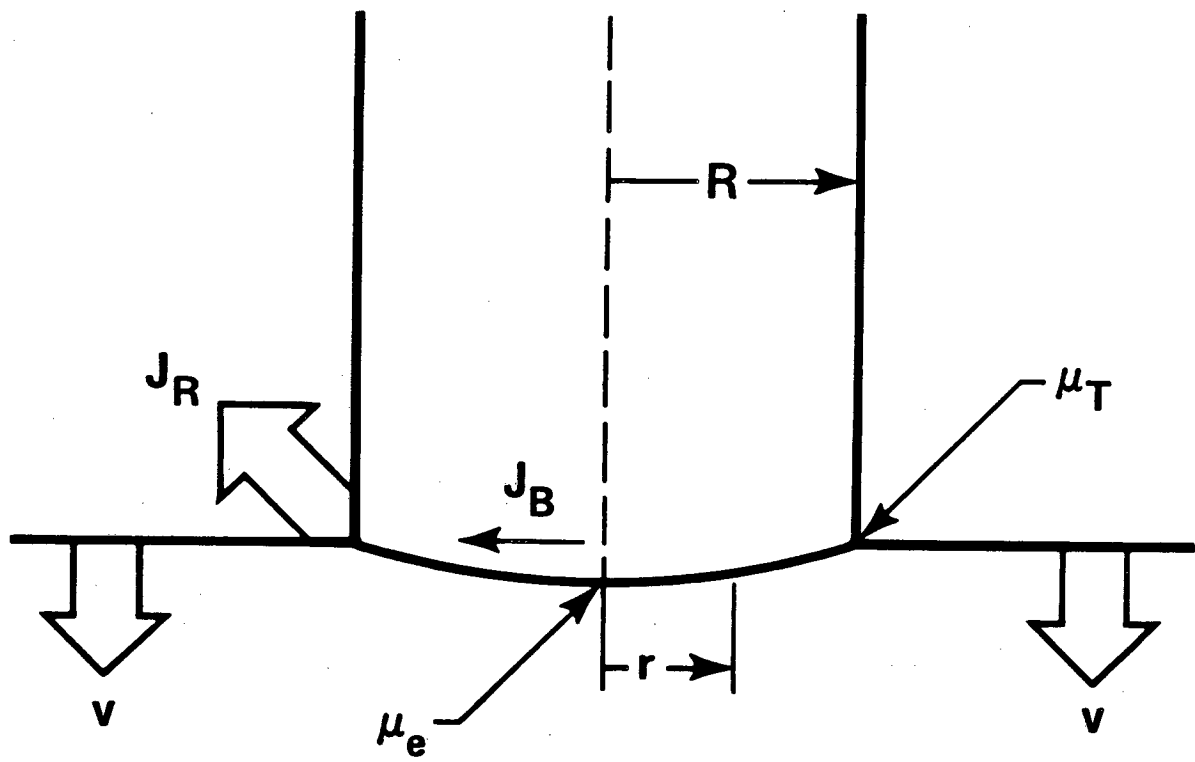
XBB 832-1366

Fig. 10



XBL 831-1142

Fig. 11



XBL 831-1139A

Fig. 12

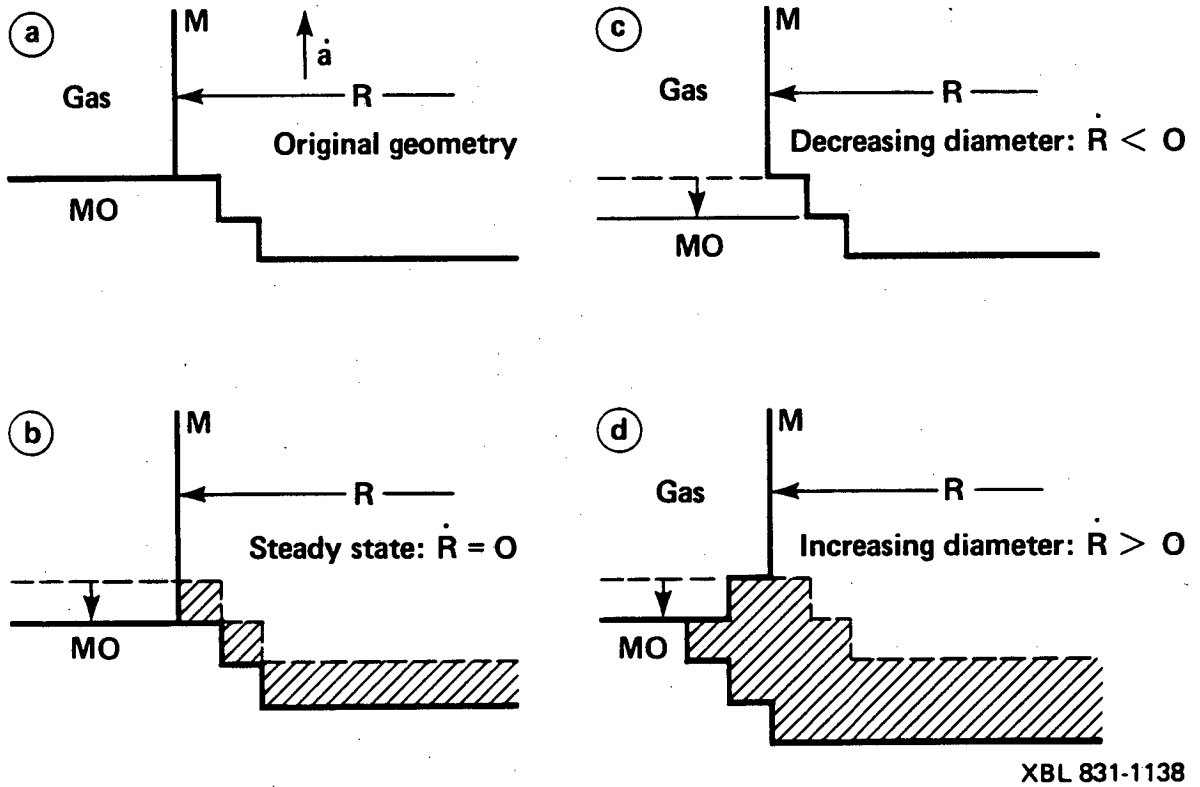


Fig. 13

This report was done with support from the Department of Energy. Any conclusions or opinions expressed in this report represent solely those of the author(s) and not necessarily those of The Regents of the University of California, the Lawrence Berkeley Laboratory or the Department of Energy.

Reference to a company or product name does not imply approval or recommendation of the product by the University of California or the U.S. Department of Energy to the exclusion of others that may be suitable.

TECHNICAL INFORMATION DEPARTMENT
LAWRENCE BERKELEY LABORATORY
UNIVERSITY OF CALIFORNIA
BERKELEY, CALIFORNIA 94720